The Use of a New Thiadiazole Derivative as a Highly Efficient and Durable Copper Inhibitor in 3.5% NaCl Solution

Fubin Ma[1,2,3], Weihua Li[1,2,], Huiwen Tian[1,2], Baorong Hou[1,2]*

[1]Key Laboratory of Marine Environmental Corrosion and Bio-fouling, Institute of Oceanology, Chinese Academy of Sciences, Qingdao 266071, China
[2] Cooperative Innovation Center of Engineering Construction and Safety in Shandong Blue Economic Zone, Qingdao 266033, China
[3]University of Chinese Academy of Sciences, Beijing 100049, China
[*]E-mail: liweihua@qdio.ac.cn

The corrosion inhibition of a newly synthesized derivate of thiadiazole (5-Methyl-[1, 3, 4] thiadiazol-2-ylsulfanyl)-acetic acid (4-hydroxy-3-methoxy-benzylidene)-hydrazide （MAH） was studied. Its inhibition performance for copper in 3.5% NaCl solution under the conditions of different pH and immersion time at 298K was investigated by weight loss, electrochemical measurements, and SEM analysis. Results show that MAH acts as a mixed-typed inhibitor, suppressing the charge transfer process by chemisorption which follows Langmuir isotherm. The compound exhibits a great potential for an excellent copper inhibitor of eco-friendliness, high efficiency and long-term durability under various pH conditions, especially in alkaline environment.

1. INTRODUCTION

Copper and its alloys are extensively utilized to fabricate structures and components such as electronics, mechanics and facilities due to their excellent electrical and thermal conductivity, mechanical properties and stability, especially the resistance towards the corrosion of many chemicals. They are widely used for wires/sheets, water pipelines, shipbuilding, seawater desalination and heat exchange systems. However, they are susceptible to corrosion in aggressive media containing chlorides, sulphates, or nitrates ions, especially in marine environment [1-7]. The corrosion issues can bring about heavy economic losses and casualties. Therefore, the control of corrosion for copper based materials in chloride containing media has been an important subject worthy of intensive researches

[8-11]. Among the protection strategies for copper corrosion such as cathodic protection, coating and conversion film technologies, the addition of corrosion inhibitors is one of the simplest and the most effective and economic means [12-14].

On the studies of copper corrosion inhibitors, there are two principle research trends. On one hand, researches on the inhibition mechanism for copper inhibitors become more and more intensive, which aims at explaining the nature of the inhibition precisely and accurately [15-20]; on the other hand, the demand for the development of eco-friendly corrosion inhibitors with low cost and high efficiency which can be used in practical engineering is more and more urgent [21-27]. However, due to their poor adaptability and poor durability, the inhibition efficiencies of many corrosion inhibitors are limited under specific conditions. For example, some inhibitors work efficiently only under a narrow pH range; when the pH changes, the inhibition efficiency decreases greatly. Some inhibitors function well during a short period of time, and don't possess long-term durability [28-32]. Thus, it is necessary to development eco-friendly inhibitors of high efficiency, good adaptability and durability.

From the perspective of efficiency and eco-friendliness, some organic compounds containing O, N, or S heteroatoms and/or π-system heterocyclic groups have been studied as effective copper inhibitors [33, 34]. These compounds are able to suppress the corrosion process by the compact film which adsorbs on the surface and blocks the active sites [35-38]. Various kinds of inhibitors like azole and thiazole derivatives, cryteine and substituted uracil, quinolines and Schiff bases are developed [39-44]. In our previous work, several kinds of organic compounds including five green triazole fungicides and two thiadiazole derivatives have been studied as highly efficient and eco-friendly copper inhibitors in synthesized seawater [45, 46].

In the present work, a new thiadiazole derivative namely (5-Methyl-[1,3,4]thiadiazol-2-ylsulfanyl)-acetic acid (4-hydroxy-3-methoxy-benzylidene)-hydrazide was synthesized. Its inhibition properties for copper in 3.5% NaCl solution under the conditions of pH ranged from 5.5 to 9.5 and immersion time from hours to a month were studied thoroughly and systematically through weight loss, potentiodynamic polarization, electrochemical impedance methods and SEM analysis. Furthermore, its adsorption isotherm was simulated and thermodynamic parameters were calculated to briefly introduce the adsorption and inhibition mechanism.

2. EXPERIMENTAL

2.1 Synthesis of MAH

The studied (5-Methyl-[1,3,4]thiadiazol-2-ylsulfanyl)-acetic acid (4-hydroxy-3-methoxy-benzylidene)-hydrazide (MAH) was synthesized in our laboratory according to the route shown in Fig.1 and characterized by proton Nuclear Magnetic Resonance spectra (^{1}H-NMR):

Molecular formula:$C_{13}H_{14}O_3N_4S_2$, ^{1}H NMR(CDCl$_3$ 500MHZ): $\delta = 2.40$ (s, 3H, -CH$_3$), $\delta = 4.06$ (s, 2H, -SCH$_2$-), $\delta = 8.49$ (s, 1H, -NH-),$\delta = 8.15$ (s, 1H, -CH=N-),$\delta = 3.84$ (s, 3H, -OCH$_3$), $\delta = 9.53$ (s, 1H, -OH), $\delta = 6.91$-7.76(m, 7H, -ArH). The ^{1}H-NMR spectrum data indicates that the compound MAH has been synthesized.
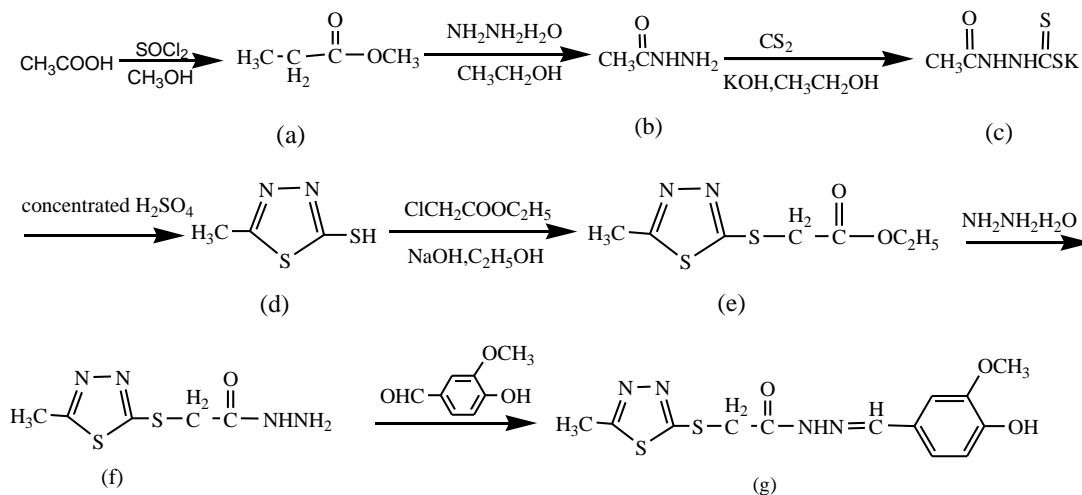
Figure 1. Synthesis route of (5-Methyl-[1,3,4]thiadiazol-2-ylsulfanyl)-acetic acid 4-hydroxy-3-methoxy-benzylidene)-hydrazide (MAH)

2.2 Materials and sample preparation

The optimized molecular structure of MAH simulated by Hyperchem software is showed in Fig.2. The studied solutions were prepared from 2.5% microemulsion of MAH. In concentration studies, the concentrations of MAH in 3.5% NaCl solution ranged from 5 mg/L to100 mg/L (pH=7.5, 298K). In pH studies, the pH of the solution ranged from 5.5 to 9.5 (298K), which was adjusted by HCl and NaOH, and the concentration of MAH was 50 mg/L. In durability studies, the immersion time ranged from an hour to 30 days with the concentration of 50 mg/L (pH=7.5, 298K). The solution in the absence of MAH was taken as blank for comparison. Three parallel experiments were performed under the same condition for each test. All the solutions were prepared with Milli-Q water (18.2MΩ·cm).
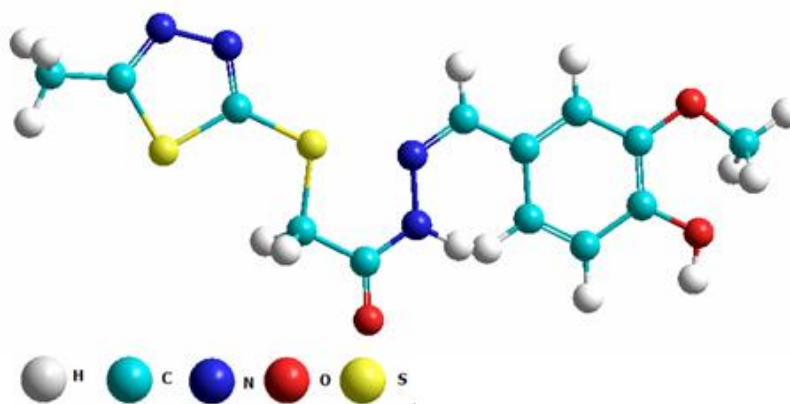
Figure 2. The optimized molecular structure of MAH

The copper specimens (purity: 99.9999%) for weight loss experiments were mechanically cut into 3.00cm×1.50cm×1.50cm in dimensions with an exposed total area of 22.20cm^2. For

electrochemical experiments, the specimens of 1.00cm×1.00cm×1.00cm were embedded in epoxy resin with a square surface area of 1.00cm^2 exposed to the electrolyte. Before all the measurements were conducted, the specimens were polished with emery paper from 1000 to 2000 grit, then rinsed ultrasonically with ethanol, acetone and copious amounts of Milli-Q water, and finally dried at room temperature.

2.3 Electrochemical experiment

Electrochemical experiments were conducted using PARSTAT 2273 Potentiostat/Galvanostat (Princeton Applied Research) with a three-electrode cell system. The copper specimens with an exposed area of 1.00cm^2 (1.00cm×1.00cm) and a platinum foil of 2.25cm^2 (1.50cm×1.50cm) were used as the working electrode and the counter electrode, respectively. A saturated calomel electrode (SCE) with a Luggin capillary was used as the reference electrode. All potentials were quoted versus SCE, and all the tests were performed in non-deaerated solutions.

Electrochemical impedance spectroscopy (EIS) measurements were carried out when the corrosion potential was stable at the open circuit potential (OCP). The used AC frequency ranged from 100 kHz to 0.01Hz with a 10 mV peak-to-peak sine wave as the excitation signal. In potentiodynamic polarization measurements, the potential was scanned from -250 mV to +250 mV (versus OCP) at a scan rate of 0.5mV/s. All the electrochemical data were collected and analyzed by PowerSuite and ZSimpWin software.

2.4 Weight loss experiment

Weight loss experiments were performed at 298K for 7 days in 3.5% NaCl solution with and without MAH. The weight loss experiment was used to evaluate the mean corrosion rate (v, gm^{-2} h^{-1}) and the inhibition efficiency (IE_w) over the exposure time was calculated by Equation 1 and 2.

$$v = \frac{W_0 - W_1}{s \times t} \qquad (1)$$

$$IE_W \% = \frac{v_0 - v_1}{v_0} \times 100\% \qquad (2)$$

where W_0/W_1 was the weight of the specimens before and after the experiment, respectively, g; s was the surface area of the specimens, m^2; t was the immersion time, h; and v_0/v_1 was the mean corrosion rates without and with MAH, respectively.

2.5 SEM analysis

The surface morphology of the specimens before and after the immersion in 3.5% NaCl solution with and without MAH were observed by Scanning Electron Microscopy (JEOL-JSM-5600) which was equipped with an Energy Dispersive X-ray spectrometer OXFORD Link-ISIS-300. The elements were detected by EDX analysis.

3. RESULTS AND DISCUSSION

3.1 Effect of the concentration

3.1.1 Potentiodynamic polarization

Fig.3 shows the polarization curves for copper in 3.5% NaCl solution at 298K in the absence and presence of different concentrations of MAH (from 5 to 100 mg/L). It is obvious that as the concentration of MAH increases, the corrosion potentials slightly shift towards the positive direction and the polarization curves move directly to much lower current densities. This indicates that the corrosion rate of copper has been reduced significantly. From the anodic and cathodic Tafel curves, it can be observed that the anodic process in the solution is effectively retarded by the inhibitor, and becomes more pronounced when increasing the concentration. Compared with the blank solution，though the cathodic current density is reduced by suppression of the reaction rate, the cathodic curve is almost parallel with each other, which indicates that the mechanism of cathodic reaction is not changed.
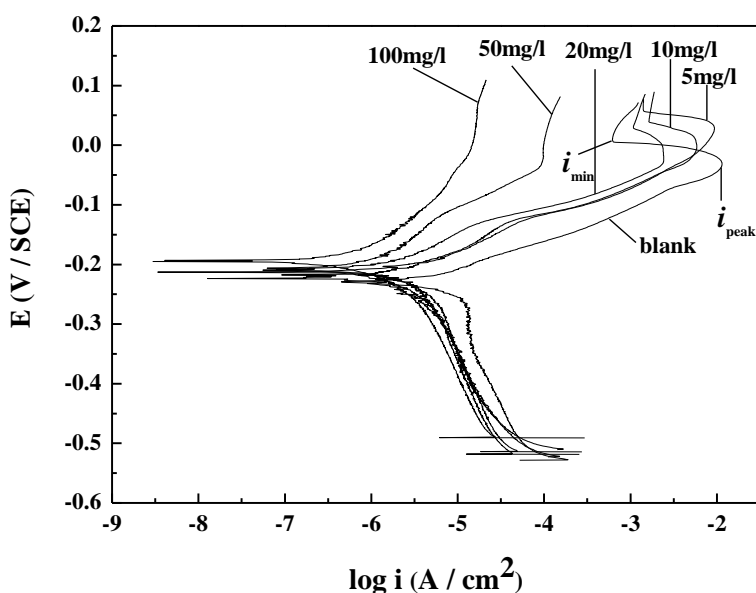
Figure 3. Polarization curves for copper in 3.5% NaCl solution with different MAH concentrations

Generally, the cathodic reaction process of copper in chloride containing solution is oxygen reduction reaction (3) [47, 48]:

$$O_2 + 2H_2O + 4e^- \rightarrow 4OH^- \qquad (3)$$

It can be proved by a little higher pH after the experiments.

The anodic reaction can be generally explained as reactions (4), (5) and (6). [4, 49, 50]. The first step is the oxidation of Cu^0 to Cu^+. Cu^+ is produced and the current density increases. Then, under the attack of the Cl⁻, Cu^+ rapidly reacts with Cl⁻ and transforms to an insoluble film CuCl. The Cu^+ is

consumed. Finally, however, due to the poor stability of CuCl, it immediately transforms to soluble cuprous chloride complex $CuCl_2^-$ shown in reaction (6). Thus, the dissolution of copper occurs step by step.

$$Cu \rightarrow Cu^+ + e^- \qquad (4)$$
$$Cu^+ + Cl^- \rightarrow CuCl \qquad (5)$$
$$CuCl + Cl^- \rightarrow CuCl_2^- \qquad (6)$$
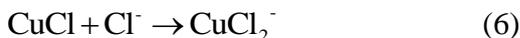
According to reactions (4) and (5), when the production rate of Cu+ is larger the consumption rate, a peak value (i_{peak}) of current density appears. And the current density begins to increases due to reaction (6). In polarization curves the change of the current densities could be observed easily. As shown in Fig.3, in the controlled experiment, i_{peak} can be obviously observed on the curve marked with blank. However, with increasing concentration of MAH, i_{peak} becomes smaller, and then completely vanishes when the concentration of MAH reaches 100mg/L. It indicates that the addition of the inhibitor reduces the active corrosion sites thus lessening the production of Cu^+ and diminishing $i_{peak.}$ As the concentration of Cl- is unchanged, the reaction processes (5) and (6) are not affected. It can be concluded that due to the adsorption of MAH on the copper surface, the reaction processes of corrosion are suppressed.

Table 1. Polarization parameters for copper in 3.5% NaCl solution with different MAH concentrations at 298K

C (mg/L)	i_{corr} ($\mu A\ cm^{-2}$)	E_{corr} (mV)	β_c (mV s^{-1})	β_a (mV s^{-1})	IE(%)
0	4.05	-218	177.20	47.60	/
5	0.830	-212.95	18.69	17.52	78.73
10	0.728	-222.55	29.34	25.27	82.03
20	0.478	-208.23	29.43	25.82	88.28
50	0.256	-206.55	31.58	30.23	93.67
100	0.175	-193.82	21.19	21.77	95.67

The electrochemical parameters such as corrosion potential (E_{corr}), corrosion current density (i_{corr}), anodic and cathodic Tafer slopes (β_a, β_c) obtained from the polarization curves are listed in Table 1. It can be observed that i_{corr} decreases significantly in the presence of the inhibitor and becomes smaller with increase of the concentration. E_{corr} shifts slightly in the positive direction, and all the shift values are less than 85mV, indicating that the inhibitor acts as a mixed-type corrosion inhibitor and plays a part in both the anodic and cathodic processes [51]. The variation of β_a and β_c also suggests that both anodic and cathodic processes are suppressed by the adsorption of MAH. The inhibition efficiency can be calculated by Equation 7 [52].

$$IE_i\% = \frac{i^0_{corr} - i_{corr}}{i^0_{corr}} \times 100\% \qquad (7)$$

Where i^0_{corr} and i_{corr} are the corrosion current densities in the absence and presence of different concentrations of MAH in 3.5% NaCl solution, respectively. The calculated inhibition efficiencies are

very high ranged from 78.73% to 95.67%, and the maximum value is 95.67% when the concentration is 100mg/L.

3.1.2. Electrochemical impedance spectroscopy (EIS)

Nyquist plots of copper in 3.5% NaCl solution with different concentrations of MAH are shown in Fig. 4. The high frequency part of Nyquist plots is given as an enlarged scale in the insert. From Fig. 4 it could be observed that the impedance spectra plots exhibit depressed capacitive loops, whose diameter increases obviously with increasing concentration of the inhibitor. It suggests that the corrosion process is mainly controlled by the charge transfer process and the corrosion resistance of copper has been enhanced significantly.
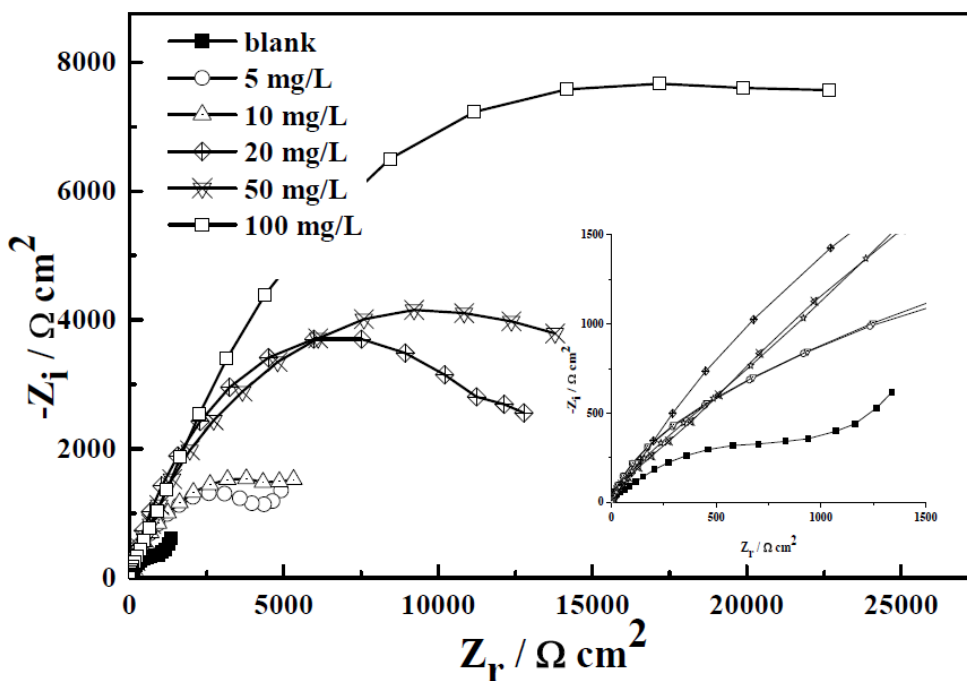
Figure 4. Nyquist plots for copper in 3.5% NaCl solution with different MAH

The impedance data could be explained using the equivalent circuit shown in Fig. 5 [53]. The electrochemical element R_s represents the resistance of the solution between the working electrode and the reference electrode. R_f represents the resistance of the film formed on the copper surface. R_{ct} represents the charge transfer resistance of corrosion process. Constant phase element Q_1 is composed of the membrane capacitance C_f of the corrosion process and the deviation parameter n_1. The capacitance C_f mainly origins from the dielectric property of surface film (corrosion products and/or inhibitor film). Q_2 is composed of the double-layer capacitance C_{dl} and the deviation parameter n_2. n represents the CPE exponent which is related with the degree of surface inhomogeneity [54]. The

surface inhomogeneity results from surface roughness, inhibitor adsorption, porous layer formation, etc.
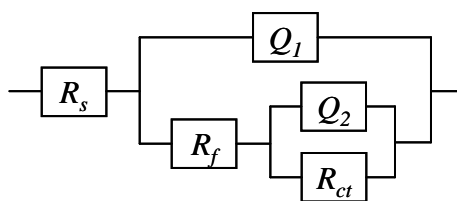
Figure 5. Equivalent circuit model to fit EIS experiment data

The parameters of the fitted equivalent circuit for copper are listed in Table 2. It shows that the film resistance R_f increases while C_f decreases apparently as the concentration of MAH increases. It suggests that a protective adsorption film is well formed on the copper/solution interface. As a result, the corrosion process of copper is greatly prevented. Moreover, R_{ct} increases remarkably with increasing inhibitor concentration, while C_{dl} tends to decrease. According to the Helmholtz model, C_{dl} is expressed as [55]:

$$C_{dl} = \frac{\varepsilon^0 \varepsilon}{d} A \qquad (8)$$

where d is the thickness of the protective layer, A is the surface area of the copper electrode, ε^0 is the vacuum permittivity, and ε is the local dielectric constant. The decrease of C_{dl} mainly results from the increase in the adsorption film area which decreases the electrode surface area (A), the decrease of the local dielectric constant (ε), and the increase in the thickness of the protective layer (d). According to the Nyquist plots and the equivalent circuit model, the inhibition reaction is mainly controlled by the charge transfer process. Thus, the inhibition efficiency obtained from EIS measurements can be calculated (Equation 9):

$$IE\% = \frac{R_{ct} - R^0_{ct}}{R_{ct}} \times 100\% \qquad (9)$$

where R^0_{ct} and R_{ct} are the charge transfer resistance without and with MAH, respectively. Compared with the solution without the inhibitor, the inhibition efficiencies calculated from R_{ct} are enhanced significantly and increase notably with the concentration of MAH. The maximum value is 96.72% when the concentration reaches is 100mg/L. It is suggested that due to the adsorption of MAH on copper/solution interface the corrosion reactions have been inhibited remarkably.

Table 2. Impedance parameters for copper in 3.5% NaCl solution with different MAH concentrations

C (mg/L)	R_s (Ω cm^2)	Q_1 (μF cm^{-2})	R_f (Ω cm^2)	Q_2 (μF cm-2)	R_{ct} (Ω cm^2)	IE (%)
0	1.301	247	43.31	455	1109	/
5	1.646	9.38	63.33	164	6214	82.15
10	1.402	8.96	70.39	71.86	8717	87.29
20	1.318	7.82	198.6	56.77	14120	92.15
50	1.314	4.59	336.7	52.11	18680	94.06
100	0.980	1.86	352.6	13.11	33780	96.72

3.1.3 Weight loss measurements

The concentration effect of MAH on copper corrosion in 3.5% NaCl solution was studied through weight loss measurements at 298K during 7 days' immersion. The corrosion rate and inhibition efficiency obtained from the measurements are listed in Table 3. It shows that after the addition of the inhibitor, the corrosion rate decreases significantly, and the corrosion current density decreases as the concentration increases from 5mg/L to 100mg/L. The inhibition efficiency increases greatly, which indicates that MAH has good corrosion inhibition performance for copper in 3.5% NaCl solution. The maximum efficiency is 95.53% at 100mg/L. These results show good agreement with those obtained from both the polarization curves and EIS. Both the electrochemical experiments and weight loss experiments prove that MAH has a great potential for a highly efficient copper inhibitor.

Table 3. Weight loss results for copper in 3.5% NaCl solution with different MAH concentrations at 298K for 7 days

C (mg/L)	$v(gm^{-2}h^{-1})$	$IE_w\%$
0	13.47	/
5	3.175	76.44
10	2.018	85.02
20	1.177	91.27
50	0.916	93.20
100	0.602	95.53

3.1.4 SEM analysis

Fig. 6 presents the SEM topography of the copper specimens before and after the immersion in 3.5% NaCl solution with and without MAH. Compared with the specimen before the immersion (Fig 6(a)), the specimen in the absence of the inhibitor (Fig 6(b)) is severely corroded by NaCl solution and a lot of local corrosion pits and a rough surface can be observed easily. However, the copper surface in the presence of 50mg/L MAH is smooth with few pits, indicating that the surface is well protected from corrosion. Because the thickness of the adsorption film is estimated to be only several nanometers, it is not apparently observed on the copper surface [23, 56]. The EDS analysis of the copper surface was conducted. Compared with the specimen without MAH, the elements including C, N, O, S are easily observed on the surface in the presence of the inhibitor. It suggests that MAH have directly adsorbed onto the copper surface and have a strong ability to suppress the corrosion of the copper.
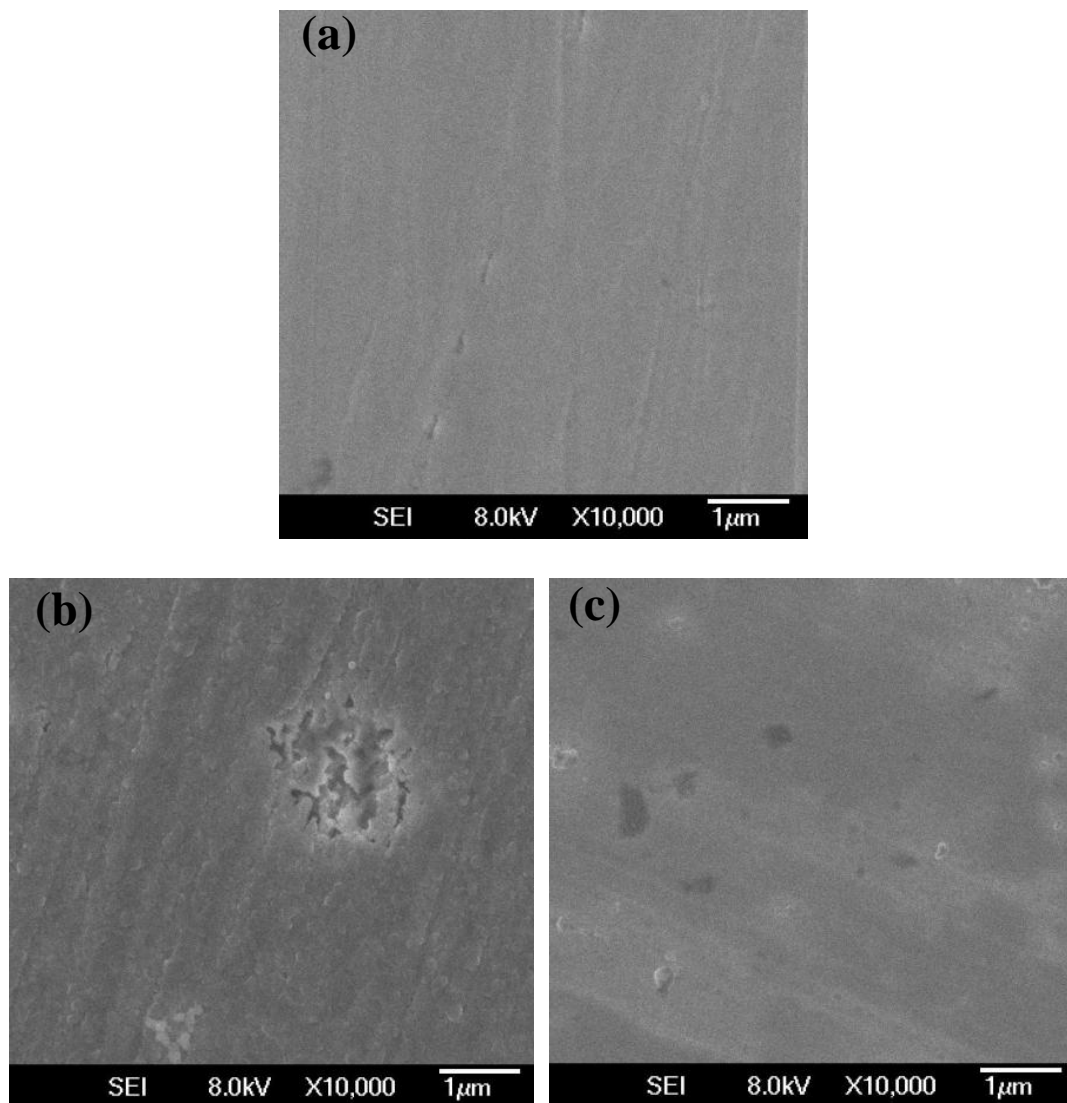
Figure 6. SEM morphology of the copper specimens: (a) before the immersion, (b) after the immersion in 3.5 % NaCl solution without MAH, (c) after the immersion in 3.5 % NaCl solution with 50mg/L MAH

3.1.5 Adsorption isotherm

The adsorption isotherm is to investigate the adsorption mechanism of the inhibitor. The data obtained from electrochemical measurements and weigh loss measurements are involved to fit the adsorption isotherm, respectively. The surface coverage θ in the Equation 10 is defined as the inhibition efficiency. Several adsorption isotherms such as Langmuir, Temkin, and Frumkin isotherms are considered to determine the best fit for θ [57]. The results show that the Langmuir isotherm and the data match well, and Langmuir isotherm is shown in Equation 10.

$$\frac{C}{\theta} = C + \frac{1}{K_{ads}} \qquad (10)$$

where K_{ads} represents the equilibrium constant of the adsorption process, C represents the concentration of the inhibitor.
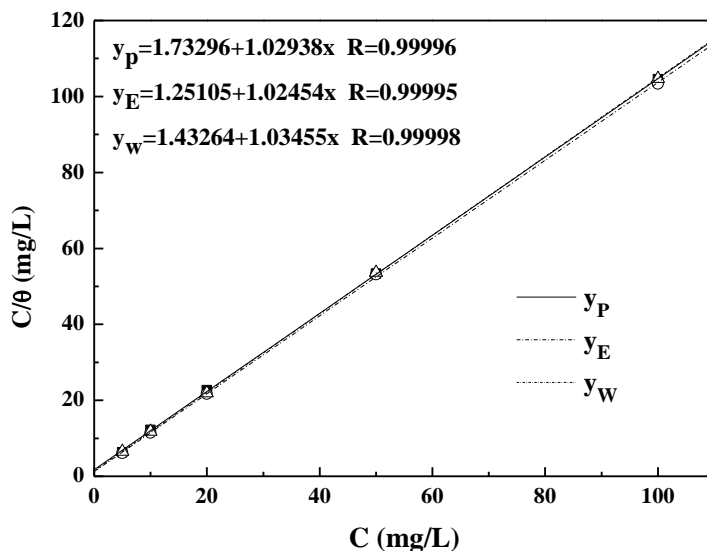
Figure 7. Langmuir adsorption isotherm of MAH on copper surface in 3.5% NaCl solution at 298K

The linear-relationship between C/θ and C is plotted in Fig. 7. It can be observed that three fitted lines are in good agreement. The subscripts (p, E, W) represent the measurements of the polarization, EIS and weight loss. The slope of C/θ versus C and the linear correlation coefficients (R) are very close to 1, indicating that the adsorption of MAH on the copper surface at 298K obeys Langmuir isotherm quite well. The free adsorption energy (ΔG^0_{ads}) can be calculated from Equation 11[58, 59].

$$K_{ads} = \frac{1}{55.5}\exp\left(-\frac{\Delta G^0_{ads}}{RT}\right) \qquad (11)$$

Thermodynamic parameters of these three experiments for Langmuir isotherm are obtained and listed in Table 4.

Table 4. Thermodynamic parameters of the adsorption in 3.5% NaCl solution

Method	K_{ads} (10^3L/mol)	ΔG^0_{ads} （kJ/mol）
Polarization	1738.10	-45.55
EIS	2886.19	-46.81
Weight loss	598.36	-42.91

It shows that the values of ΔG^0_{ads} are all negative, which indicates that the adsorption of MAH on the surface in 3.5% NaCl solution is spontaneous. Though there is a little difference between the values of ΔG^0_{ads} calculated from different measurements, they are all in the range of 42-46kJ/mol, which is regarded as the chemisorption. In chemisorption process, the inhibitor takes action by the covalent bond formed by the sharing charge or charge transfer process. While in physisorption process, the value of ΔG^0_{ads} is about 20kJ/mol or lower, and the inhibitor functions by the electrostatic

interactions between the charged molecule and the metal [60, 61, 62]. The results confirm that the adsorption of MAH on copper surface is chemisorption and the interaction between the inhibitor molecules and the copper surface is the covalent bond. The formed adsorption film is compact and is likely to protect the copper effectively, efficiently, and durably.

3.2 Effect of pH

3.2.1. Potentiodynamic polarization
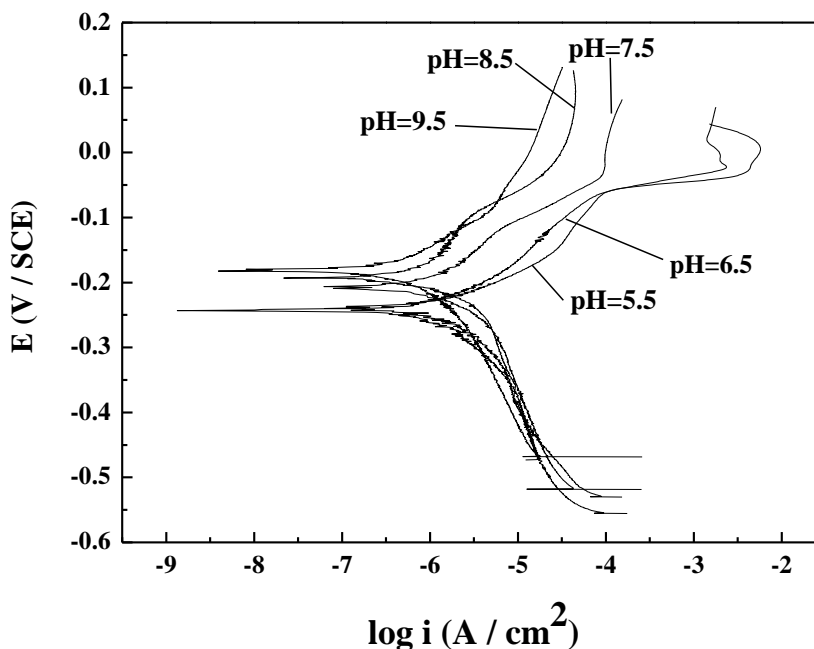
Figure 8. Polarization curves for copper in 3.5% NaCl solution with 50mg/L MAH under different pH conditions at 298K

In the studied pH range, the curves without MAH are very close to each other, so only one curve is used for comparison in Fig. 8. Polarization curves and polarization parameters for copper in 3.5% NaCl solution with 50mg/L MAH under different pH conditions at 298K are shown in Fig. 7 and in Table 5. Under the studied pH conditions, the corrosion current densities (i_{corr}) decrease greatly in the presence of the inhibitor. In the pH range from 5.5 to 9.5, 50mg/L MAH shows good inhibition performance for copper in 3.5% NaCl solution. The corrosion potentials (E_{corr}) shift slightly in the positive direction compared with the blank, and the variation of β_a and β_c also confirms that both the dissolution of copper and oxygen reduction processes are restrained by the presence of the inhibitor. The efficiencies increase gradually with increasing pH. The maximum efficiency is 97.12% at pH=9.5 and the efficiency order under different pH conditions is 9.5>8.5>7.5>6.5>5.5. It suggests that the corrosion resistance of copper with MAH under alkaline condition is better than that under near neutral or acidic conditions.

Table 5. Polarization parameters for copper in 3.5% NaCl solution with 50mg/L MAH under different pH conditions at 298K

pH	i_{corr} (μA cm^{-2})	E_{corr} (mV)	βc (mV s^{-1})	βa (mV s^{-1})	IE(%)
5.5	0.479	-241.86	30.13	30.58	88.17
6.5	0.284	-243.73	22.69	24.03	92.98
7.5	0.256	-206.55	21.58	22.23	93.67
8.5	0.238	-192.85	22.27	22.48	94.12
9.5	0.117	-181.78	20.27	21.80	97.12

3.2.2. Electrochemical impedance spectroscopy (EIS)
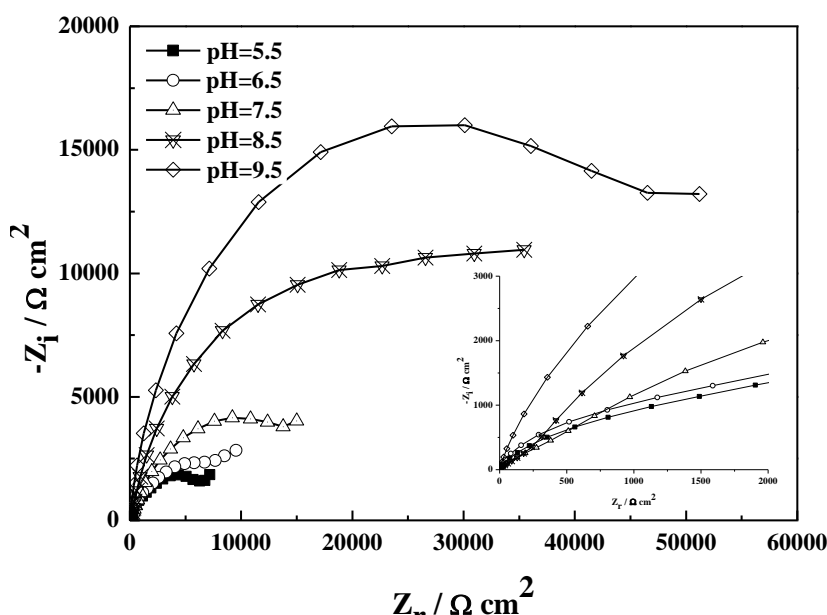
Figure 9. Nyquist plots for copper in 3.5% NaCl solution with 50mg/L MAH under different pH conditions at 298K

Nyquist polts of copper in 3.5% NaCl solution under different pH conditions without and with inhibitors are shown in Fig.9. It can be observed that the diameter of the depressed capacitive loop increases greatly in the presence of MAH compared with the blank and it increases with increase of pH. According to the equivalent circuit (Fig. 5), the impedance data is fitted and the electrochemical parameters are listed in Table 6. Under the studied pH ranged from 5.5 to 9.5, R_{ct} increases significantly while C_{dl} decrease greatly. It also reveals that the charge transfer process of the corrosion reaction under various pH conditions is inhibited effectively by the protective adsorption film on the interface. It is inferred that under alkaline conditions excessive hydroxide ions could promote Cu^+/Cu^{2+} transforming into copper hydroxides and cuprous/copper oxides which have protective effect on the copper; at the same time, they also suppress the cathodic reaction [28, 63-65]. The inhibition efficiencies in the studied pH range are very high, and the maximum value of the inhibition efficiency is 98.50% when pH is 9.5. The efficiency order is 9.5>8.5>7.5>6.5>5.5, which is consistent with the

results obtained from the polarization curves. It could be concluded that the inhibitor can be used under a wide pH ranges (pH=5.5 to 9.5), and shows a better performance under alkaline conditions.

Table 6. Impedance parameters for copper in 3.5% NaCl solution with 50mg/L MAH under different pH conditions at 298K

pH	R_s (Ω cm^2)	Q_1 (μF cm^{-2})	R_f (Ω cm^2)	Q_2 (μF cm^{-2})	R_{ct} (Ω cm^2)	IE (%)
5.5	1.07	4.03	58.30	119.2	9266	89.11
6.5	2.11	1.42	56.34	103.5	15307	92.78
7.5	1.31	1.86	98.64	71.9	18680	94.06
8.5	1.89	1.30	77.65	34.4	38930	97.15
9.5	2.01	1.51	80.29	20.1	74080	98.50

3.2.3 Weight loss experiment

In the pH experiments, the mean corrosion rate is measured by weight loss experiment and the results are shown in Table 7. In the studied pH ranges, the inhibitor shows good inhibition performance and all the inhibition efficiencies are over 85%. Under alkaline conditions (pH=8.5, 9.5), the efficiency is higher. The order of the efficiency uder different pH conditions is 9.5>8.5>7.5>6.5>5.5. These results are in good agreement with the results obtained from those of the electrochemical experiments.

Table 7. Weight loss experiments in 3.5% NaCl solution with different pH at 298K

pH	v (10^{-5} g m^{-2} h^{-1})	IE%
blank	13.47	/
5.5	1.852	86.25
6.5	1.668	87.62
7.5	0.683	94.93
8.5	0.533	96.04
9.5	0.416	96.91

3.3 Effect of immersion time

The effect of the immersion time on copper corrosion in 3.5% NaCl solution in the presence of 50mg/L MAH at 298K and pH=7.5 is studied by EIS measurements. The obtained Nyquist plots during 30 days' immersion are shown in Fig. 10, and the corresponding electrochemical parameters are listed in Table 8. It can be observed that in the early days, R_{ct} fluctuates to some extent, but remains a high value all the same and the inhibition efficiencies are very high. When the immersion time lasts for 30 days, the inhibition efficiency reaches 99.98%. These results suggest that a compact protective adsorption film can rapidly forms on the copper surface, and the film has a good inhibition

performance [17]. As the time goes on, the film keeps intact and has a excellent protection effect towards corrosion. The results reveal that the inhibitor has a great potential to be used as a long-lasting and highly efficient corrosion inhibitor for copper.
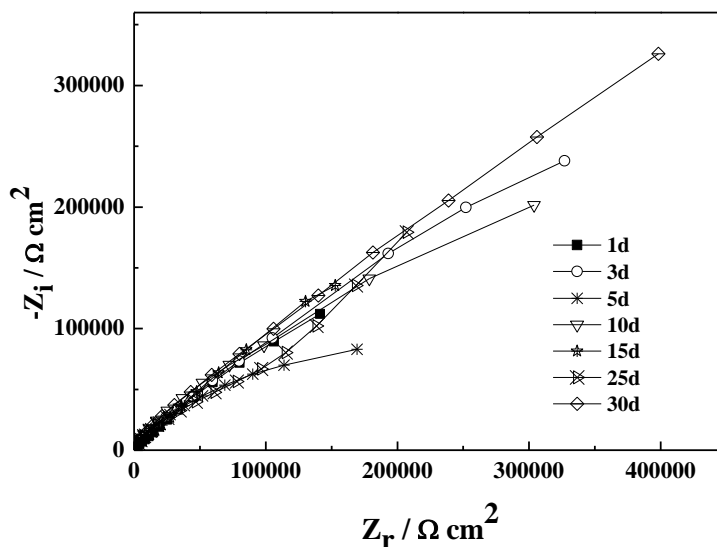
Figure 10. Nyquist plots for copper in 3.5% NaCl solution with 50mg/L MAH during the 30 days' immersion

Table 8. Impedance parameters for copper in 3.5% NaCl solution with 50mg/L MAH during the 30 days' immersion

Time (day)	R_s (Ω cm^2)	Q_1 (μF cm^{-2})	R_f (Ω cm^2)	Q_2 (μF cm^{-2})	R_{ct} (Ω cm^2)	IE (%)
1	2.98	1.66	4154	20.3	1037000	99.89
3	3.67	2.05	1963	10.3	951800	99.88
5	4.29	2.97	4095	11.6	463700	99.76
10	3.84	3.71	1950	10.1	696400	99.84
15	3.76	4.22	2331	32.6	234300	99.53
25	3.59	0.96	4123	3.84	87540	98.73
30	6.09	0.75	1768	6.16	5542000	99.98

4. CONCLUSIONS

The inhibition performance of the newly synthesized MAH on the corrosion of copper in 3.5% NaCl solution under different pH and immersion time conditions has been studied systematically, and these conclusions can be acquired:

1. In the concentration range of 5-100mg/L, MAH shows a good inhibition performance for copper in 3.5% NaCl solution. MAH acts as a mixed-typed inhibitor which suppresses both the anodic and cathodic process by chemisorption on the copper surface, and its adsorption obeys Langmuir adsorption isotherm.

2. Under the studied pH range from 5.5 to 9.5, MAH shows slightly different but high inhibition efficiencies. Higher efficiencies are acquired under alkaline conditions than those under neutral and acidic conditions. The efficiency order under various pH conditions is: 9.5>8.5>7.5>6.5>5.5.

3. Due to the rapid adsorption and high inhibition efficiency of MAH, the effect of immersion time on the inhibition performance is not obvious, and generally the efficiencies are very high. MAH shows a good durability for the protection of copper in 3.5% NaCl solution.

4. MAH has a great potential to be used as a copper inhibitor of environment-friendliness, high efficiency and long-term durability under various pH conditions, especially in alkaline environment.

References

1. A. Drach, I. Tsukrov, J. DeCew, J. Aufrecht, A. Grohbauer, U. Hofmann, *Corros. Sci.*, 76 (2013) 453.
2. S. H. Lee, J. G. Kim, J. Y. Koo, *Eng. Fail. Anal.*, 17 (2010) 1424.
3. F.M. AlKharafi, N.A. Al-Awadi, I.M. Ghayad, R. M. Abdullah and M. R. Ibrahim, *Int. J. Electrochem. Sci.*, 6 (2011) 1562.
4. G. Kear, B.D. Barker, F.C. Walsh, *Corros. Sci.*, 46 (2004) 109.
5. L. Nunez, E. Reguera, F. Corvo, E. Gonzalez, C. Vazquez, *Corros. Sci.*, 47 (2005) 461.
6. A. A. EI Warraky, H. A. EI Shayeb, E. M. Sherif, *Anti-Corros. Methods Mater.*, 51 (2004) 52.
7. N. Huynh, S.E. Bottle, T. Notoya, D.P. Schweinsberg, *Corros. Sci.*, 42 (2000) 259.
8. M. M. Singh, R. B. Rastogi, B. N. Upadhyay, M. Yadav, *Mater. Chem. Phys.*, 80 (2003) 283.
9. N. Bellakhal, M. Dachraoui, *Mater. Chem. Phys.*, 85 (2004) 366.
10. M. M. Antonijevic, S. M. Milic, M. B. *Petrovic, Corros. Sci.*, 51 (2009) 1228.
11. M. Finsgar, I. Milosev, *Corros. Sci.*, 52 (2010) 2737.
12. D. Gelman, D. Starosvetsky, Y. Ein-Eli, *Corros. Sci.*, 82 (2014) 271.
13. Z. Chen, L. Huang, G. Zhang, Y. Qiu, X. Guo, *Corros. Sci.*, 65 (2012) 214.
14. C. W. Yan, H. C. Lin, C. N. Cao, *Electrochim. Acta*, 45 (2000) 2815.
15. M. Itagki, M. Tagaki, K. Wantanabe, *Corros. Sci.*, 38 (1996) 601.
16. A. G. Christy, A. Lowe, V. Otieno-Alego, M. Stoll, R. D. Webster, *J. Appl. Electrochem.*, 34 (2004) 225.
17. M. Finšgar, *Corros. Sci.*, 72 (2013) 90.
18. M. Finšgar, D. K. Merl, *Corros. Sci.*, 80 (2014) 82.
19. P. Song, X. Y. Guo, Y. C. Pan, S. Shen, Y. Sun, Y. Wen, H. F. Yang, *Electrochim. Acta*, 89 (2013) 503.
20. Sudheer, M.A. Quraishi, *Corros. Sci.*, 70 (2013) 161.
21. M. Scendo, *Corros. Sci.*, 47 (2005) 1738.
22. M. Scendo, *Corros. Sci.*, 50 (2008) 1584.
23. M. Finšgar, *Corros. Sci.*, 77 (2013) 350.

24. D. Gopi, K. M. Govindaraju, V. Collins Arun Prakash, D. M. Angeline Sakila, L. Kavitha, *Corros. Sci.*, 51 (2009) 2259.
25. B. Trachli, M. Keddam, H. Takenouti, A. Srhiri, *Corros. Sci.*, 44 (2002) 997.
26. C. C. Li, X. Y. Guo, S. Shen, P. Song, T. Xu, Y. Wen, H. F. Yang, *Corros. Sci.*, 83 (2014) 147.
27. G. M. Abd El-Hafez, W. A. Badawy, *Electrochim. Acta*, 108 (2013) 860.
28. H. Otmcic Curkovic, E. Stupnisek Lisac, H. Takenouti, *Corros. Sci.*, 52 (2010) 398.
29. G. Tansuğ, T. Tüken, E. S. Giray, G. Fındıkkıran, G. Sığırcık, O. Demirkol, M. Erbil, *Corros. Sci.*, 84 (2014) 21.
30. Y. H. Wang, J. B. He, *Electrochim. Acta*, 66 (2012) 45.
31. G. Quartarone, M. Battilana, L. Bonaldo, T. Tortato, *Corros. Sci.*, 50 (2008) 3467.
32. N. Kovačević, A. Kokalj, *Corros. Sci.*, 73 (2013) 7.
33. Zarrouk, B. Hammouti, H. Zarrok, M. Bouachrine, K.F. Khaled, S.S. Al-Deyab, *Int. J. Electrochem. Sci.*, 7 (2012) 89.
34. M. Finšgar, A. Lesar, A. Kokalj, I. Milošev, *Electrochim. Acta,* 53 (2008) 8287.
35. W. H. Wang, Z. Li, Q. Sun, A. J. Du, Y. L. Li, J. Wang, S. W. Bi, P. Li, *Corros. Sci.*, 61 (2012) 101.
36. L. Romanszki, I. Datsenko, Z. May, J. Telegdi, L. Nyikos, W. Sand, *Bioelectrochemistry*, 97 (2014) 7.
37. K. Y. Zhang, L. D. Wang, G. C. Liu, *Corros. Sci.*, 75 (2013) 38.
38. A. Zarrouk, B. Hammouti, R. Touzani, S.S. Al-Deyab, M. Zertoubi, A. Dafali, S. Elkadiri, *Int. J. Electrochem. Sci.*, 6 (2011) 4939.
39. W. H. Li, X. Bai, F. K. Yang, B. R. Hou. *Int. J. Electrochem. Sci.*, 7 (2012)2680.
40. K. M. Ismail, *Electrochim. Acta*, 52 (2007) 7811.
41. A. Dafali, B. Hammouti, R. Mokhlisse, S. Kertit, *Corros. Sci.*, 45 (2003) 1619.
42. J. M. Bastidas, P. Pinilla, E. Cano, J. L. Polo, S. Miguel, *Corros. Sci.*, 45 (2003) 427.
43. H. O. Curkovic, E. Stupnisek Lisac, H. Takenouti, *Corros. Sci.*, 51(2009) 2342.
44. H. Y. Ma, S. Chen, L. Niu, S. S. Zhao, S. Li, D. C. Li, *J. Appl. Electrochem.*, 32 (2002) 65.
45. W. H. Li, L. C. Hu, S. T. Zhang, B. R. Hou, *Corros. Sci.*, 53 (2011) 735.
46. H. W. Tian, W. H. Li, K. Cao, B. R. Hou, *Corros. Sci.*, 73 (2013) 281.
47. E. M. Sherif, S. M. Park, *J. Electrochem. Soc.*, 152 (2005) B428.
48. E. S. M. Sherif, *Appl. Surf. Sci.*, 252 (2006) 8615.
49. H. O. Curkovic, E. Stupnisek Lisac, H. Takenouti, *Corros. Sci.*, 52 (2010) 398.
50. T. Tuken, N. Kicir, N. T. Elalan, G. Sigircik, M. Erbil, *Appl. Surf. Sci.*, 258 (2012) 6793.
51. A. K. Satapathy, G. Gunasekaran, S. C. Sahoo, K. Amit, P. V. Rodrigues, *Corros. Sci.*, 51 (2009) 2848.
52. K. F. Khaled, *Electrochim. Acta*, 54 (2009) 4345.
53. Q.A. Huang, R. Hui, B. Wang, J. Zhang, *Electrochim. Acta*, 52 (2007) 8144.
54. L. J. Li, X. P. Zhang, J. L. Lei, J. X. He, S. T. Zhang, F. S. Pan, *Corros. Sci.*, 63 (2012) 82.
55. I. Ahamad, R. Prasad, M. A. Quraishi, *Corros. Sci.*, 52 (2010) 1472.
56. M. Finšgar, D. Kek Merl, *Corros. Sci.*, 83 (2014) 164.
57. P. M. Krishnegowda, V. T. Venkatesha, P. K. M. Krishnegowda, S. B. Shivayogiraju, *Ind. Eng. Chem. Res.* 52 (2013) 722.
58. M. Scendo, *Corros. Sci.*, 49 (2007) 373.
59. F. Bentiss, M. Lebrini, M. Lagrenée, M. Traisnel, A. Elfarouk, H. Vezin, *Electrochim. Acta*, 52 (2007) 6865.
60. M. A. Hegazy, A. M. Badawi, S. S. Abd El Rehim, W. M. Kamel, *Corros. Sci.*, 69 (2013) 110.
61. M. Behpour, S. M. Ghoreishi, N. Soltani, M. Salavati Niasari, M. Hamadanian, A. Gandomi, *Corros. Sci.*,50 (2008) 2172.
62. H. W. Tian, W. H. Li, B. R. Hou, *Int. J. Electrochem. Sci.,* 8 (2013) 8513.
63. M. S. El-Sayed, *Int. J. Electrochem. Sci.*, 7 (2012) 2832.

64. M. B. P. Mihajlović, M. M. Antonijević. *Int. J. Electrochem. Sci.*, 10 (2015) 1027.
65. H. Baeza, M. Guzman, R. Lara. *Int. J. Electrochem. Sci.,* 8 (2013) 7518.